Annual Review of Biophysics

Split Green Fluorescent Proteins: Scope, Limitations, and Outlook

Matthew G. Romei and Steven G. Boxer

Department of Chemistry, Stanford University, Stanford, California 94305, USA;
email: mromei@stanford.edu, sboxer@stanford.edu

Annu. Rev. Biophys. 2019. 48:19–44

First published as a Review in Advance on February 20, 2019

The *Annual Review of Biophysics* is online at biophys.annualreviews.org

https://doi.org/10.1146/annurev-biophys-051013-022846

Keywords

split protein, green fluorescent protein, bimolecular fluorescence complementation, biosensor, photochemistry

Abstract

Many proteins can be split into fragments that spontaneously reassemble, without covalent linkage, into a functional protein. For split green fluorescent proteins (GFPs), fragment reassembly leads to a fluorescent readout, which has been widely used to investigate protein–protein interactions. We review the scope and limitations of this approach as well as other diverse applications of split GFPs as versatile sensors, molecular glues, optogenetic tools, and platforms for photophysical studies.

Contents

1. INTRODUCTION

1.1. Ribonuclease S—the First Split Protein

The earliest example of a split protein is ribonuclease S, discovered by Fred Richards (113). Richards was interested in the effects of nucleases on protein structure and found that ribonuclease A—then, one of the best studied enzymes and the subject of the classic demonstration by Anfinsen that a protein can spontaneously fold—was cut by subtilisin at a single site. Despite the cut, the protein remarkably retained its enzymatic activity, implying that the cut fragments had a high affinity [dissociation constant (K_d) of around 30 pM]. X-ray crystallography showed no loss of secondary or tertiary structure (156). The cut site, between residues 20 and 21, is a loop region between the N-terminal α-helix and the rest of the protein (113). The two fragments could be separated, yielding the S-peptide (residues 1–20) and the S-protein (residues 21–124). Each fragment was shown to be disordered in solution. The removal of the S-peptide disrupts enzymatic activity, as the cut site removes residues that are essential for activity, and activity is fully restored upon readdition of the S-peptide at a 1:1 ratio. The importance of this observation in the early days of understanding protein structure and folding cannot be overstated (5).

1.2. General Features and Purposes of Split Proteins

The two essential features of all split proteins are (*a*) a lack of activity of each fragment in the absence of the other and (*b*) the restoration of activity upon fragment complementation or reconstitution. If the fragments are expressed in vivo, each must be stable to proteolytic digestion. In

most cases, the split site lies in a loop between well-defined secondary structural features. In some cases, the purpose of splitting a protein is to study factors that influence the binding of peptides to proteins, while in others, it is to introduce noncanonical amino acids on a peptide [a recent example uses ribonuclease S (31)] or, in the case of split green fluorescent protein (GFP), to detect the interactions of proteins fused to the split fragments by GFP fluorescence (38).

1.3. Nonfluorescent Split Proteins and Protein-Fragment Complementation Assays

A remarkable array of proteins has been split over the past six decades for a diverse range of applications. Soon after the first report of ribonuclease S (113), similar studies examined protein folding and elucidated structure–function relationships of β-galactosidase and staphylococcal nuclease fragments (132, 142). The approach proved to be quite general and was applied to address universal questions about protein folding (37) and even extended to investigate protein evolution (8, 129). Analogous protein fragmentation and complementation techniques are still employed today, as in the study of the structure and mechanism of transmembrane ion channels (3, 102, 120).

The original example of a conditional split protein complementation system was reported by Johnsson & Varshavsky (50), who demonstrated that ubiquitin fragments only reassembled into an active protease tag when fused to two interacting proteins (a leucine zipper homodimer). This pivotal split ubiquitin system laid the foundation for all future protein-fragment complementation assays (PCAs) that link the function of a split reporter protein to a specific protein–protein interaction (PPI) (**Figure 1**). Conceptually, any protein whose activity results in a clear and measurable readout can act as the reporter in a PCA. To date, many proteins, such as ubiquitin (50), β-galactosidase (118), dihydrofolate reductase (104), β-lactamase (36), firefly luciferase (81), TEV protease (152), thymidine kinase (84), Cas9 (160), horseradish peroxidase (83), RNA polymerase (106), and aminoacyl tRNA synthetase (134), have been engineered as split PCA reporters to detect both transient and irreversible PPIs. The types of readouts for these assays include fluorescence, bioluminescence, cell survival, gene transcription, protein translation, positron emission, genome editing, and electron microscopy. Since this review focuses on split fluorescent proteins (FPs) and their numerous and often overlooked applications, we refer the interested reader to earlier, thorough reviews for more details about the properties and scope of split nonfluorescent proteins (85, 89, 90, 127, 153, 154).

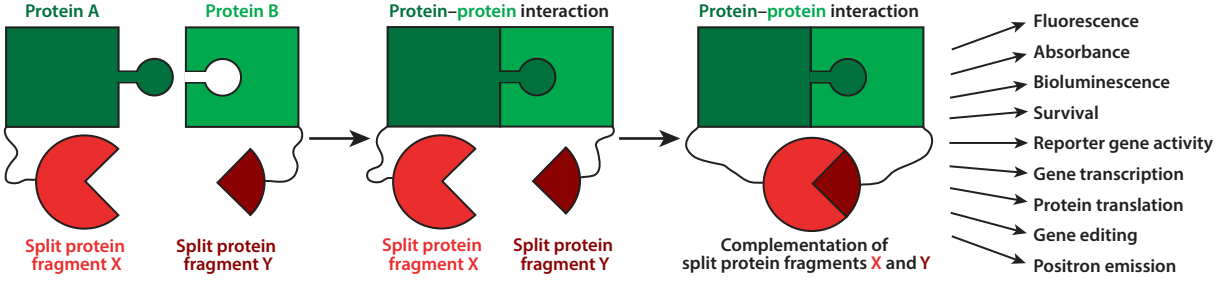

Figure 1

General schematic of protein-fragment complementation assays. The engineered split protein fragments X and Y (shown in shades of *red*) are genetically fused to two proteins whose interaction is of interest (proteins A and B, shown in shades of *green*). Upon interaction of proteins A and B, the effective concentration of the split protein fragments increases such that fragments X and Y form a noncovalently bound complex and regain native activity, creating the assay's protein–protein interaction–dependent readout.

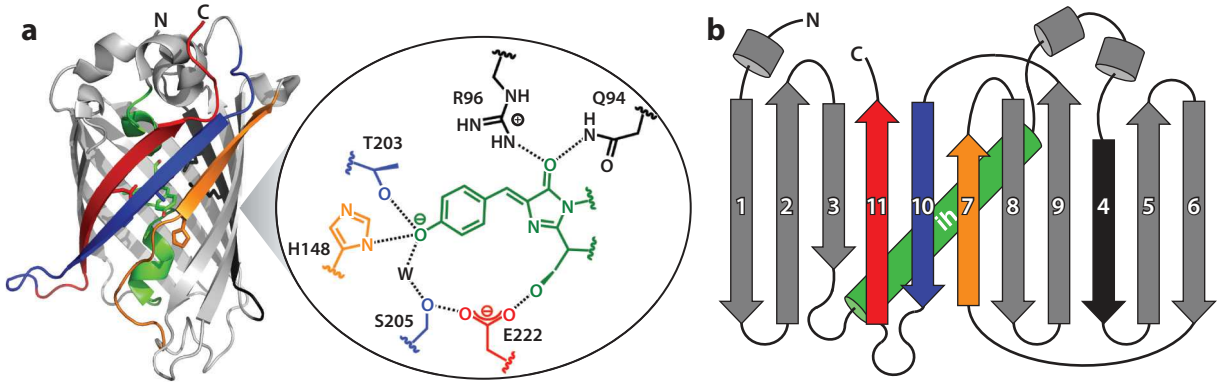

Figure 2

Green fluorescent protein (GFP) structure and topology. (*a*) Ribbon structure of GFP (PDB ID: 2B3P) (103) highlighting the chromophore environment and the proximity of the N- and C-termini. The internal α-helix that contains the chromophore is shown in green, while β-strands 4, 7, 10, and 11 are shown in black, orange, blue, and red, respectively. (*b*) Topology of GFP's 11 β-strands and internal α-helix (ih). Figure adapted with permission from Reference 78.

2. GREEN FLUORESCENT PROTEIN

2.1. GFP Structure, Chromophore Maturation, and Photophysical Properties

GFP is the most widely used genetically encoded fluorescent reporter. The history and engineering of GFPs have been extensively reviewed (1, 22, 23, 93, 100, 110, 111, 115, 125, 140, 164). Here, we focus on critical aspects of the protein topology, folding, chromophore maturation, and chromophore photophysical properties that inform the design and properties of split versions of GFP. The iconic 11-stranded β-barrel structure of GFP is shown in **Figure 2*a***, along with the strand topology in **Figure 2*b***. Colors in **Figure 2** designate β-strands 4, 7, 10, and 11 (the C-terminal strand) that contain most of the amino acids that contact the chromophore and affect its color and excited-state properties. The internal α-helix (ih), shown in green, contains amino acids 65–67 that become the chromophore. Amino acids Q94 and R96, shown in black, as well as E222, shown in red, are important for chromophore maturation.

The chromophore maturation process is critical for any imaging application of GFP and especially for split GFPs. Since the pioneering work of Tsien and colleagues (40) and Reid & Flynn (109), which was then further elaborated by Getzoff and colleagues (7) and Wachter and colleagues (117), it is widely accepted that chromophore formation is an autocatalytic cyclization and oxidation of the S-Y-G sequence; this process can occur only within the folded protein. Oxygen is essential for chromophore maturation, and much work has improved the maturation rate from hours in the original jellyfish protein (40) to minutes in the fastest maturing forms (29, 103, 124). Many amino acid substitutions have been made in and near the chromophore that affect its color and pK_a (acid dissociation constant).

The chromophore itself is essentially nonfluorescent in fluid solution. Studies of the isolated model chromophore *p*-hydroxybenzylidenedimethylimidazolinone (HBDI) suggest that the primary nonradiative decay pathway is *cis-trans* isomerization, and this pathway is greatly inhibited either in frozen solution or in a confined space. The remarkable RNA aptamer Spinach was selected to bind tightly to a modified free GFP chromophore, 3,5-difluoro-4-hydroxybenzylidenedimethylimidazolinone (DFHBDI), and other related nonfluorescent chromophores rendering them fluorescent by impeding photoisomerization (99); a split version

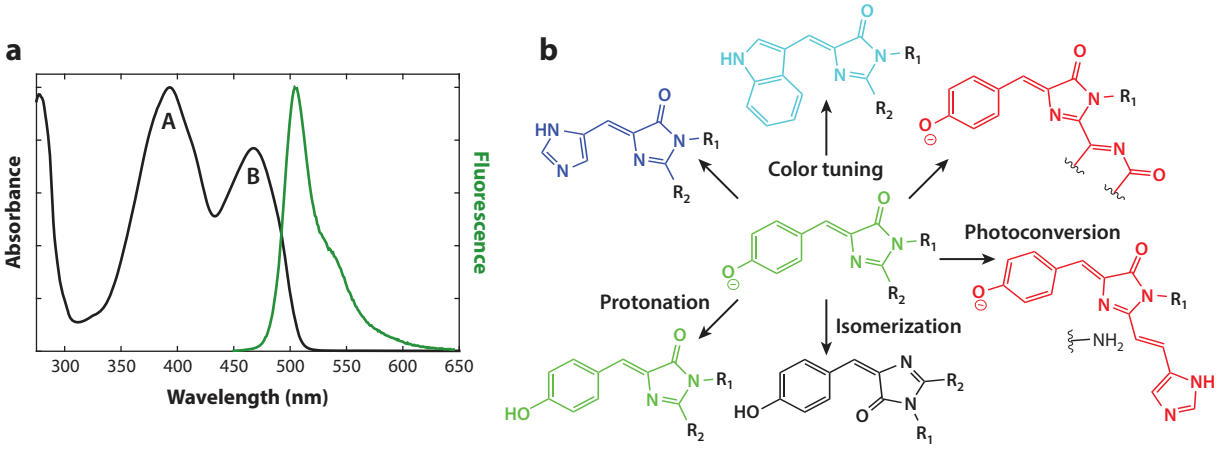

Figure 3

Photophysical properties of the green fluorescent protein (GFP) chromophore. (*a*) Absorbance (*black*) and fluorescence emission (*green*) spectra of superfolder GFP (S65) (59). The protonated A state and deprotonated B state absorb at 393 and 467 nm, respectively. (*b*) Several factors influence the structure and photophysical properties of the GFP chromophore. Mutations to Y66 and nearby residues can tune chromophore absorption and fluorescence across the visible spectrum. Modulating the chromophore's pK_a (acid dissociation constant) is beneficial for various microscopy applications and biosensor development. In most reversibly switchable fluorescent proteins, the chromophore isomerizes from the fluorescent *cis* to the nonfluorescent *trans* conformation when irradiated with blue light. The chromophore then undergoes either thermal relaxation or violet light–driven isomerization back to its original state. Finally, the chromophore can convert to a red fluorescent species from a green fluorescent precursor (termed photoconversion) or convert to a fluorescent species from a nonfluorescent precursor (termed photoactivation; not shown).

of Spinach has been made to probe nucleic acid–nucleic acid interactions (64, 116). The chromophore exists in either a protonated or deprotonated form (typically called A state and B state, respectively), as shown in the absorption spectrum in **Figure 3*a*** (16). This feature allows GFP to function as a pH sensor whose pK_a depends on many factors, including the amino acids that comprise the chromophore and closely interacting amino acids such as H148 and T203 (**Figure 2*a***). Depending on the construct, some GFP chromophores are sensitive to pH while others are surprisingly buffered against pH changes (96). The most commonly used forms of GFP are derived from the S65T mutation in which the chromophore is found almost exclusively in the deprotonated (B state) form at physiological pH.

2.2. Circular Permutation and GFP Engineering

As seen in **Figure 2*a***, the C- and N-termini of GFP are spatially adjacent, making it straightforward to circularly permute the sequence such that any of the 11 β-strands or the internal α-helix can become the new C- or N-terminus. GFP has proven to be extremely robust to circular permutation, and engineered forms of GFP often use circularly permuted variants as starting points (4, 139). Many sensor designs are based on circular permutation and the insertion of entire foreign protein sequences (28, 115). GFP is also extremely tolerant of mutations, and vast numbers of changes have been made to affect expression, color, stability, chromophore maturation rate, and capacity for photoswitching, photoactivation, and photoconversion (**Figure 3*b***). Superfolder GFP is a particularly useful variant selected for high stability (103). Extensive protein engineering has generated a wide array of red fluorescent proteins (RFPs) originating from

diverse natural sources and producing a remarkable range of colors (115, 128). The great advantage of RFPs is their red-shifted absorption, which allows greater penetration of light into tissues and minimizes autofluorescent background, but the altered spectral properties typically come with a more complex chromophore maturation process (typically via a green intermediate) and a reduction in fluorescence quantum yield compared with GFPs. To date, there are fewer examples of split RFPs (**Table 1**).

Table 1 Existing split fluorescent proteins with relevant properties

Split fluorescent protein[a]	Fluorescence excitation/emission maxima (nm)	Split site residue number (β-strand)[c]	Application notes	Reference(s)
SCFP3A	433/474	N 1–173 (8), C 156–239 (7)	PPI	145
sCFP1,2	433/475–476	214 (10)	SR	70
ECFP	452/478	154 (7); 172 (8)	PPI	44
Cerulean	439/479	154 (7)	PPI	131
Gmars-T (mMaple)	476/498	164 (8)	PPI, SR	148
rsEGFP2	478/503	158 (7)	PPI, SR	149
GFP (sg100)	475/505	157 (7)	PPI	38
sfGFP	485/507	214 (10); 193 (9), 212 (10)	PPI	11, 13
Folding reporter GFP	485/507	157 (7)	PPI	122
EGFP	488/507	158 (7)	PPI	112
mKusabira-Green	494/507	168 (8)	PPI	141
mKusabira-Green2	494/507	169 (8)	PPI	69
sGFP1,2,3	485–491/508–510	214 (10)	SR	70
mTSapphire	399/511	154 (7)	PPI	150
Photoactivatable GFP	475/517	(7)	PPI, SR	157
Dronpa	503/517	164 (8); 181 (9)	PPI, SR	41, 75
mNeonGreen2	ND	213 (10)	Imaging	33
sYFP1,2,3	509–515/522–524	214 (10)	SR	70
UnaG	497/527	84 (NA[d])	PPI[e], exo	138
EYFP	515/527	154 (7); 155 (7); 172 (8)	PPI	43, 44, 146
Venus	515/527	154 (7); 172 (8); 210 (10)	PPI	41, 94, 131
sfYFP	515/527	154 (7)	PPI	97
Citrine	516/529	154 (7)	PPI	131
mKusabira-Orange2	551/565	154 (7)	PPI	35
mRFP1	549/570	154 (7)	PPI	47
mIris	546/578[b]	150 (7)	PPI, SR	17
mEos3.2	570/580[b]	164 (8)	PPI, SR	80
dsRed monomer	558/583	168 (8)	PPI	68
CyOFP1	488–526/589	151 (7)	PPI	150
mScarlet-I	569/593	159 (7)	PPI	151
PAmCherry1	564/595[b]	159 (7)	PPI, SR	92
FusionRed	577/606	188 (9)	PPI	73
mCherry	587/610	159 (7)	PPI	30

(*Continued*)

Table 1 (*Continued*)

Split fluorescent protein[a]	Fluorescence excitation/emission maxima (nm)	Split site residue number (β-strand)[c]	Application notes	Reference(s)
sfCherry	ND	208 (10)	Imaging	53
sfCherry2	ND	208 (10)	Imaging	33
PAsfCherry2	ND	208 (10)	SR	33
mPlum	570/615	23 (1)	PPI	54
mLumin (mKate)	587/621	151 (7)	PPI	19
mNeptune	600/650	155 (7)	PPI	39
miRFP670	642/670	122 (NA[d])	PPI, exo	126
IFP1.4	684/708	132 (NA[d])	PPI[e], exo	133
miRFP709	683/709	122 (NA[d])	PPI, exo	126
iRFP	690/713	119 (NA[d])	PPI, exo	34

Abbreviations: exo, exogenous chromophore responsible for fluorescence; NA, not applicable; ND, not determined; PPI, detection of protein–protein interactions; SR, super-resolution imaging.

[a]Sorted by fluorescence emission maximum.

[b]Upon photoactivation or photoconversion.

[c]Protein split on C-terminal side of listed residue (β-strand).

[d]Not applicable, as protein structure is not comparable to that of a typical fluorescent protein.

[e]Shown to exhibit reversible PPI detection.

3. SPLIT FLUORESCENT PROTEINS AND THE DETECTION OF PROTEIN–PROTEIN INTERACTIONS

3.1. Original Design

The advent of split proteins has revolutionized the detection of protein–protein interactions, and no class of split proteins has made a greater impact than split FPs. At the turn of the twenty-first century, split protein complementation to study PPIs was limited to a few enzymes whose assays required exogenous fluorogenic substrates, highly engineered cell lines, and/or binary readouts of protein interactions. By contrast, FPs have many properties that can overcome those limitations, as they intrinsically produce a fluorescent signal proportional to the number of correctly folded proteins containing mature chromophores. Additionally, the stable and robust β-barrel structure, conserved among FPs, is tolerant of circular permutation, various peptide and protein insertions, and harsh assay conditions. With these advantages in mind, Ghosh et al. (38) developed the first example of a split FP capable of reconstitution into a fluorescent complex. The GFP variant sg100 was split at a surface loop between residues 157 and 158 (β-strands 7 and 8), creating N- and C-terminal fragments of 157 and 81 residues, respectively. The split GFP fragments were genetically fused to separate leucine zipper domains that associate to form an antiparallel heterodimer. When either refolded in vitro from denaturation conditions or coexpressed in *Escherichia coli*, the resulting fusion proteins reassembled into a noncovalently bound fluorescent heterodimer, suggesting that the two GFP fragments were able to reconstitute into a native-like structure that favored chromophore maturation. Importantly, in the absence of the leucine zipper domains or either single GFP fragment, no fluorescence was observed, indicating that the interaction of the fusion proteins is essential to reconstitute fluorescence from the two nonfluorescent fragments. This foundational work demonstrated the ability to detect PPIs through a conditional reassembly of split fluorescent protein fragments.

3.2. Bimolecular Fluorescence Complementation

Recognizing the utility and potential of the discovery by Ghosh et al., many labs began to expand on the original split FP assay. The use of split FPs became so prevalent that a PCA with a split FP reporter was given a unique name: bimolecular fluorescence complementation (BiFC). BiFC can investigate PPIs in vivo with the capacity to image subcellular PPI localization in a variety of hosts, including bacteria, mammalian cells, plant cells, tissues, and live animals. Since complementation of two FP fragments is an irreversible process in almost all cases once chromophore maturation has occurred (see Sections 3.3 and 4.3 below), BiFC can detect weak (1 mM K_d) and transient PPIs (2, 82, 88). BiFC also benefits from comparatively small tags fused to the proteins of interest; an FP fragment can be as small as 15–20 residues (e.g., a single β-strand), which minimizes perturbations to the proteins whose interaction is being probed (11, 13). To extend the scope of the technique to include the potential for multicolor imaging, FP variants spanning a wide spectral range from the visible to the near infrared were engineered as split reporters and implemented in BiFC assays (**Table 1**), and several resources outline design principles and best practices to guide those interested in developing a new split FP (42, 63, 67, 74, 89). One particularly exciting advancement in BiFC is the extension of split reporters to FPs with unique photophysical properties such as photoactivation, photoconversion, and photoswitching (**Figure 3*b***), which allows for the combination of super-resolution imaging and PPI detection in live cells (17, 33, 41, 75, 80, 92, 148, 149, 157). The current diversity and continual innovation of split FPs is a testament to the utility of BiFC as a biochemical tool, the robustness of the conserved FP β-barrel, and the advances in molecular biology and protein engineering technologies over the past two decades.

3.3. Addressing Limitations of Bimolecular Fluorescence Complementation

Despite the clear benefits discussed above, BiFC has noteworthy drawbacks that should be carefully considered whenever performing, interpreting, or critiquing an experiment. First, while irreversible binding of split FP fragments allows for detection of weak and transient PPIs, it prevents any time-dependent study of the interaction of interest because the off-rate of the split FP with a mature chromophore is typically very low. This leads to accumulation of the fluorescent signal from the irreversible complementation that could misinform the experimentalist about the native behavior of the given PPI. Furthermore, the split FP interaction effectively stabilizes or fixes the PPI. Second, there is an unavoidable delay between the interaction of the proteins of interest and the fluorescent readout due to split FP complementation, proper protein folding, and chromophore maturation. Although several studies have reduced the time delay as discussed below, this issue still places a lower limit of minutes to hours on the time resolution of BiFC. Third, the split FP fragments have an inherent binding affinity for each other independent of the interaction of their fusion proteins (discussed further below). Nonspecific self-assembly of the FP fragments creates false positives. Therefore, careful quantitative controls are essential when implementing any BiFC experiment; this is thoroughly outlined in a few sources (42, 67, 74). Finally, BiFC is ultimately a sensor of protein–protein proximity rather than of direct interaction. Thus, a positive BiFC result may stem from shared cellular localization between two proteins or the fact that the proteins are both part of a larger complex. Neither situation necessitates a direct PPI between the proteins of interest, which may lead to misinterpretation of data.

A significant body of work is dedicated to improving three of BiFC's major limitations: (*a*) irreversible complementation, (*b*) poor complementation and chromophore maturation efficiencies, and (*c*) nonspecific self-assembly of split FP fragments. Addressing the first limitation, just two split FPs have been reported as reversible for the study of PPI dynamics, neither of which

are derived from GFP. Tchekanda et al. (133) engineered a split infrared FP from the monomeric IFP1.4, which is based on a biliverdin-containing bacteriophytochrome. The reversibility of the system was demonstrated in vitro as well as in eukaryotic cells. To expand the spectral range of reversible PPI detection, To et al. (138) designed a green split protein variant, uPPI, derived from UnaG, a member of the fatty-acid-binding protein family that binds bilirubin. Reversibility of the split uPPI complementation was demonstrated in mammalian cells using the rapamycin-dependent dimerization of FKBP and Frb. Despite the requirement for exogenous chromophores, these two reversible BiFC reporters have the potential to reveal spatiotemporal dynamics of PPIs with low background signals, a benefit not possible for any other split FPs reported to date. Note, however, that the reversibility of the system is simply based on the binding affinity of the split FP fragments. Cellular concentration of the fusion proteins and effective local concentration of the split FP fragments during the PPI of interest will therefore determine the equilibrium state of the FP complex and ultimately the applicability of the assay. Alternative systems for reversible PPI detection are reviewed in depth elsewhere (154).

Faster fluorescence responses from split FP complementation due to PPIs have been engineered to address the second limitation. These advances have greatly expanded the scope of BiFC, mitigating experimental burdens such as long incubation times, prohibitively low signals, and arduous optimization of conditions and fusion protein linkages. Despite the extraordinary impact of the original split GFP reported by Ghosh et al., fluorescence detection guided by the strong heterodimerization interaction of the leucine zipper domains was still quite slow (38). Subsequent improvements have focused on accelerating chromophore maturation by introducing mutations that facilitate protein folding at relevant physiological temperatures. The split FP fragments of Citrine, Venus, and Cerulean exhibit brighter BiFC signals than their parent proteins, enhanced yellow fluorescent protein (EYFP) and enhanced cyan fluorescent protein (ECFP); require reduced incubation times at cell culture temperatures; and eliminate the need for low-temperature incubation before imaging (131). Similarly, folding reporter GFP, a variant designed for efficient protein folding in *E. coli*, can detect weaker PPIs, while split sg100 GFP fragments show no signal in a side-by-side comparison (122).

Further efforts to shorten the assay time targeted the solubility and stability of the FP fragments within cells. Cabantous et al. (13) split the especially stable superfolder GFP in between the 10th and 11th β-strands, yielding a 214-residue N-terminal fragment (GFP1–10) and a 17-residue C-terminal peptide (GFP11, the smallest split FP fragment to date). Directed evolution of each fragment greatly improved solubility and complementation efficiency. Note that this specific split GFP system, discussed further in Section 3.4, was evolved to self-assemble and originally not used to detect PPIs. In contrast, split superfolder YFP was designed for identifying interactions in cells, during which PPI-independent self-assembly would be an unwanted event. Split between residues 154 and 155 after strand 7 and containing 15 folding- and solubility-enhancing mutations, split superfolder YFP displays a strong BiFC signal, indicating proximity of two genetically fused proteins of interest with comparably short incubation times (97).

One additional approach to reduce lengthy incubation times required in BiFC experiments evades the problem of chromophore maturation. The larger N-terminal fragment of EGFP (β-strands 1–7) was surprisingly shown by Demidov et al. (24) to contain a mature chromophore once refolded from inclusion bodies in vitro with properties similar to that of denatured EGFP. As with the free chromophore in solution, fluorescence of the fragment is very weak (∼100-fold lower than intact, folded EGFP). However, when the split fragments are fused to complementary DNA strands and mixed together, fluorescence appears within a minute, suggesting that the rate-limiting step is fragment complementation induced by DNA hybridization rather than chromophore maturation. While this particular assay is limited to in vitro studies, the phenomenon

of chromophore maturation within a split FP fragment may be more prevalent than discussed in the BiFC literature. If a 158-residue EGFP fragment maintains enough structure and sufficient contacts with neighboring residues, however transiently, to form a mature chromophore in the absence of its complementary fragment, then it is plausible that similar split protein fragments, especially larger ones that contain most of the β-strands, generate mature chromophores during other in vivo and in vitro experiments (33, 45, 46). Alternatively, chromophore maturation within a single FP fragment may be facilitated inadvertently through stabilizing intramolecular (affinity tags, fusion proteins) or intermolecular (host proteins) interactions. Nevertheless, the reduction in required incubation times for certain FP fragment pairs could be due in part to more efficient chromophore maturation before fragment complementation. This potential by-product of protein engineering is a fortuitous property that still allows for low background signal in the absence of a PPI while greatly accelerating the fluorescent readout upon split FP complementation.

Regardless of these advancements in BiFC reporters, the issue of split FP fragment self-assembly, the third limitation, still produces unwanted background fluorescence and limits the detection capabilities of the technique. The relevant parameter to consider for fragment self-assembly in vivo is the equilibrium binding constant between fragments that do not contain the mature chromophore. To our knowledge, this value has not been measured for any FP fragment pair with an immature chromophore. Alternatively, for systems intentionally evolved to self-assemble, such as GFP1–10 and GFP11, the arguably more relevant parameter to assess fragment complementation is the on-rate (note that the equilibrium constant equals the ratio between the on-rate and off-rate). For fragment pairs that contain intermediates en route to a mature chromophore, on-rates for different FP variants range from 25 to 70 M^{-1} s^{-1} (70). For fragments already containing a mature chromophore, the few reported on-rates are one to two orders of magnitude larger (25, 26, 46, 58). The corresponding equilibrium constants for fragments with a mature chromophore range from hundreds of picomolar to hundreds of nanomolar depending on the fragment pair (26, 46). While these values may give a general idea for the binding affinity of some FP fragments, the number of fragment pairs studied is quite limited and only consists of single β-strand fragments with their ten β-stranded complements. The small fragment for most BiFC reporters consists of two to four β-strands. More quantitative characterization of FP fragment properties would aid in the design of improved BiFC reporters and should be a focus of future work.

To minimize the complications from fragment self-assembly, Blakeley et al. (9) designed a split superpositive GFP in which the N- and C-terminal fragments have theoretical net charges at pH 7 of +24 and +10, respectively, compared to the −8 overall theoretical net charge of sg100 GFP. Fusion of superpositive GFP fragments to leucine zipper domains enhanced the fluorescent signal compared to both split sg100 GFP and split folding reporter GFP at physiological temperatures. Cabantous et al. (11) creatively modified their original GFP1–10/GFP11 system to generate a split FP reporter that addresses many key limitations of BiFC. Superfolder GFP was split into three fragments (GFP1–9, GFP10, and GFP11) to generate a tripartite split GFP assay that detects PPIs without temperature restrictions. This heavily engineered system provides small fusion tags (GFP10 and GFP11 are 19 and 21 residues, respectively) to avoid aggregation issues of larger fragments, minimize the perturbation to fusion proteins, and virtually eliminate background from self-assembly.

General trends in split FP properties become apparent when discussing the attempts made to engineer the optimal BiFC reporter. The vast majority of FPs are split at surface loops after β-strands 7 or 8, creating N- and C-terminal fragments with about a 2:1 size ratio. These proteins tend to exhibit reduced background from self-assembly compared with FPs split into one large fragment and one β-strand peptide though at the expense of reduced solubility and a tendency for

aggregation. Mutations that improve solubility, stability, and folding efficiency of split FP fragments lead to enhanced fluorescent signals and shorter BiFC assay incubation times, but these intended improvements often result in higher levels of background fluorescence and FP fragment self-assembly, possibly due to a combination of increased fragment affinity and availability in cells. The ideal properties of a specific split FP certainly depend on the application, but there still exists a balance between the native affinity for self-assembly of the two split FP fragments and the time between the PPI of interest and a detectable fluorescence readout, an unavoidable limitation of BiFC.

The benefits, experimental details, best practices, and applications of BiFC have been exhaustively reviewed (61–63, 67, 74, 89, 114, 130, 144, 154). Split FPs have a wide variety of additional useful, important, and creative applications that are often overlooked and not reviewed elsewhere. For the remainder of this review, we delve into the additional functions of split FPs that provide insight into basic photophysical and photochemical properties of FPs, expand the repertoire of optogenetic tools, detect proximity and localization in other molecular and cellular contexts, and offer a platform for localizing molecules of interest.

3.4. Expanding the Scope of the Split GFP Proximity Sensor

While PPI detection is their most common function, split FPs have also been used to study the proximity between and localization of other relevant biological entities. Rackham & Brown (108) pioneered a new assay called trimolecular fluorescence complementation to visualize RNA–protein interactions in live cells using the split YFP Venus. This technique was extended to detect and track RNA localization and dynamics with a range of split FP spectral variants (39, 98, 135, 143, 155, 159). By using the tripartite split GFP system in a modified RNA detection assay termed tetramolecular fluorescence complementation, Kellerman et al. were able to drastically reduce assay times and background fluorescence (55) and introduce multicolor capability to simultaneously image two RNAs (56). Another major application of the split FP proximity sensor is called GRASP, or GFP reconstitution across synaptic partners, which can detect proximity across synapses or even cell membrane contacts in live animals. Split FP fragments are each fused to transmembrane proteins such that proximity of the two cells' membranes leads to split FP complementation and subsequent fluorescence (32). A method analogous to GRASP was designed to detect and even quantify organelle proximity (21, 52).

Similar to the way intact FPs have been adapted to sense environmental stimuli, many labs have cleverly combined the utility of a fluorescent readout with FP fragment complementation to investigate important biological processes. The original GFP1–10/GFP11 system was designed to quantitatively report on the solubility of expressed proteins with a simple fluorescence measurement (14). This method was later improved to detect protein misfolding with high sensitivity by inserting the protein of interest between circularly permuted GFP fragments (12). Aggregation of proteins such as tau could also be directly probed since the higher-order aggregates sequester the fused GFP fragment and occlude binding to its complement (20). Three groups designed protease sensors that take advantage of split GFP complementation. Each strategy utilizes variations of a cyclic, locked GFP11 fragment that opens upon protease cleavage, allowing for complementation with GFP1–10 and subsequent fluorescence (15, 119, 137). Split GFP also serves as a sensor for protein kinase and phosphatase activity (158) as well as cytoplasmic delivery of cell-penetrating peptides or other cargo (86, 101, 123). To create a sensor for a unique target peptide sequence, Huang et al. (45) evolved a circularly permuted GFP variant missing its final strand to bind a peptide from influenza's hemagglutinin protein; efforts are underway to optimize the fluorescent response of this sensor upon peptide binding. The tripartite split GFP system has also been engineered to report on enzymatic activity of small GTPases and sortase (72, 161). Split FPs have

proven useful as well in high-throughput screening experiments, given their ability to screen for PPIs (48), RNA–protein interactions (57), and enhanced protein stability (79) as well as quantify each library variant's expression (121) and secretion levels (66).

Split FPs that were evolved for self-assembly (GFP1–10/GFP11 and its derivatives) have been used for targeting, localization, and imaging in various approaches. For example, Kamiyama et al. (53) used GFP11 as a multimerization scaffold to recruit the transcriptional activation domain, VP64, and enhance gene expression. With protein-based therapeutics in mind, Bale et al. (6) targeted nanoparticles to specific organelles in live cells. As imaging tools, these split FP pairs help visualize endogenous localization patterns and dynamics of proteins in live cells both with standard and super-resolution microscopy (33, 49, 51, 53, 77, 105). In another application from the Pinaud lab, split GFP links together two gold nanoparticles, with a mature GFP complex acting as the bridge, creating a photoacoustic and surface-enhanced Raman spectroscopy imaging probe. Additional functionalization of the nanoparticles targets the probe to specific cell types (71). Further engineering of GFP1–10/GFP11 allows for polymerization of the GFP fragments into both linear and cyclic supramolecular assemblies of various sizes. The assemblies can be functionalized to display other proteins of interest to study multivalent interactions, to colocalize functional proteins within cells, or to construct higher-order nanostructures (65). Finally, fusion of the strand-10 and strand-11 β-hairpin to a protein of interest and subsequent GFP1–9 complementation provides a stable, ordered fusion partner to promote more favorable protein crystallization (76, 91).

4. PHOTOCHEMICAL AND PHOTOPHYSICAL STUDIES USING SPLIT GFPs

4.1. Overall Goals of In Vitro Studies of Split GFPs

Most studies using split GFPs described in Section 3 were performed in cells and focused on detection of protein–protein interactions. As with the original work by Richards (113) on split ribonuclease, split GFPs can be used to study GFP itself. This has been the primary focus of work from our lab, which began with a simple question: If a fluorescent protein fragment is expressed in *E. coli* and isolated, can adding a synthetic peptide similar to the missing protein fragment generate a fluorescent protein? What are the limits of this approach; that is, can the protein be circularly permuted and still reassemble in vitro? If the answer is yes, then the synthetic strand could introduce any noncanonical amino acid, probe, or label [in parallel, amber suppression (147) could introduce noncanonical amino acids into the recombinantly made fragment]. Once assembled (or upon site-specific cleavage of the intact protein; see Section 4.2), such split proteins can be used to investigate kinetics and thermodynamics of peptide association, using their intrinsic absorption and fluorescence as a reporter. Furthermore, as we discovered, split GFPs exhibit some very unusual photochemical and photophysical properties that could be exploited to engineer new optogenetic tools, complementing their conventional role in imaging and potentially overcoming some of the limitations described earlier for complementation assays. Note that detailed sequence information for each construct is essential when using these systems and should always be reported.

4.2. Synthetic Control of GFPs

Our initial efforts closely followed work done in cells with split GFPs, but without any fused protein or nucleic acid partners. Kent et al. (59) expressed and isolated a recombinant protein corresponding to β-strands 1–10 [specifically, GFP1–10OPT introduced by Cabantous et al. (13)]

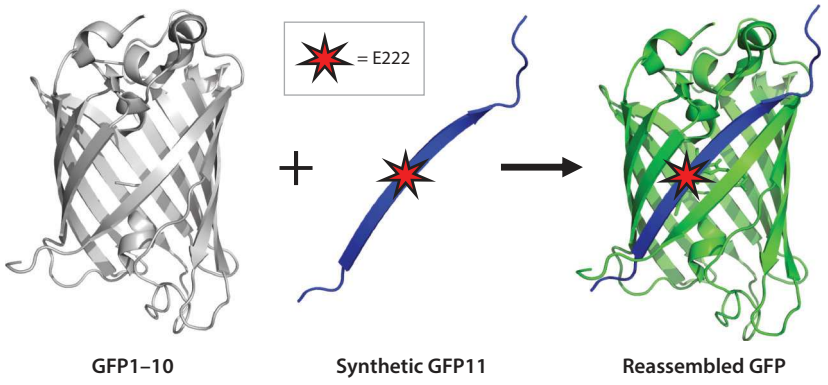

Figure 4

Schematic diagram illustrating split protein reassembly between recombinant GFP1–10 and a synthetic GFP11 peptide with subsequent chromophore maturation (PDB ID: 2B3P) (103). Mutations at E222 tune the photophysical properties of the chromophore. Note that the 3D structure of the truncated protein shown in gray is not currently known. Figure adapted with permission from Reference 59.

and added a synthetic peptide mimicking strand 11, as illustrated in **Figure 4**. GFP1–10 was found largely in inclusion bodies and was isolated by standard methods in urea and purified using a His tag on the N-terminus. Upon diluting the protein from denaturing buffer in the presence of synthetic strand 11, a fluorescent protein was formed in oxic conditions over a period of two days. Because strand 11 is tightly bound, this split semisynthetic protein could be further purified and compared with the recombinant full-length protein. The maturation of the chromophore within the protein in vitro was confirmed by electrospray mass spectrometry (the intact split protein could be observed under gentle conditions). Furthermore, the chromophore had an identical absorption spectrum to that of the full-length protein and responded similarly to mutations such as E222Q. Finally, excited-state proton transfer (16) in this semisynthetic protein was identical to that in the intact protein, assuring that molecular contacts with the chromophore were maintained.

While successful, the yield of GFP1–10 was poor, and considerable time was required for chromophore maturation. A much more direct strategy for achieving the same result is shown in schematic form in **Figure 5** (60). In this approach, a selective proteolytic cleavage site was engineered between strands 10 and 11 (**Figure 5*a***), and the entire protein was expressed in *E. coli* in high yield with a fully matured chromophore. Upon purification, these proteins can be cleaved, subjected to denaturing conditions required to remove the cleaved strand, and then recombined with a synthetic strand by diluting together from denaturing buffer. Through circular permutation, this approach can effectively exchange any secondary structural element in the GFP topology, even the chromophore-containing internal α-helix (**Figure 5*b***). Remarkably, following denaturation to remove the internal α-helix, refolding in the presence of a synthetic peptide corresponding to the internal α-helix sequence leads to formation of the native chromophore. In this case, the empty barrel catalyzes chromophore maturation, which can be exploited to modify the chromophore in ways not easily achieved by amber suppression. Furthermore, the peptide bearing the mature chromophore isolated from the recombinant protein can be inserted into an empty barrel whose sequence would hinder chromophore maturation. For example, in an effort to reverse the electric field around the chromophore, we made the R96E and E222K mutations (95). R96 and E222 (**Figure 2**) are essential for chromophore maturation, so

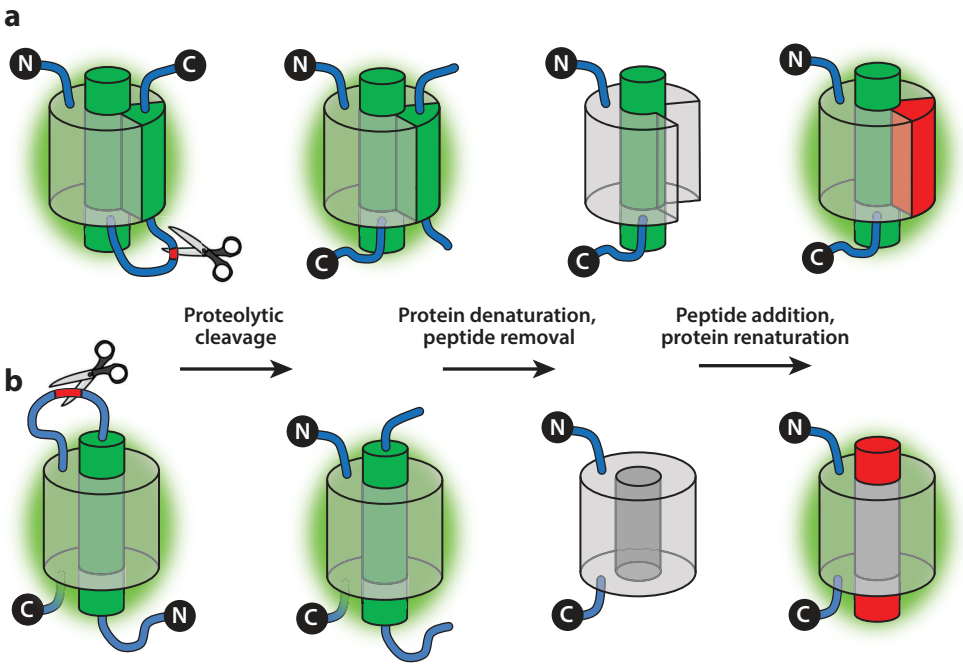

Figure 5

Schematic illustrating the required experimental steps for the synthetic control of green fluorescent protein, applied to either (*a*) the strand 7, 10, or 11 system or (*b*) the internal α-helix system. The loop between the terminal secondary structural element and the rest of the protein is proteolytically cleaved. The noncovalently bound complex is denatured, and the fragments are separated with size exclusion chromatography. Refolding of the larger fragment, referred to as the denatured truncated protein (shown in *gray* as if folded), with synthetic peptide (shown in *red*) corresponding to the missing structural element yields a fluorescent species resembling the native protein. Point mutations on the synthetic peptides that cause color shifts and/or protonation state changes can be introduced in this manner. Figure adapted with permission from Reference 60.

the above mutations would ordinarily produce protein with an immature chromophore. However, by combining an internal α-helix peptide bearing the mature chromophore created in its native environment with the R96E/E222K empty barrel, it was possible to create and study this novel protein.

4.3. Photochemistry of Split GFPs—Phenomenology

As described above, when a proteolytic cut is made between strand 11 and the rest of the protein, strand 11 remains noncovalently bound and can be removed only by denaturation (**Figure 5*a***). The rest of the protein, shown as a barrel containing ten β-strands, is referred to as the truncated protein. In contrast to the last step in **Figure 5*a***, if the truncated protein is separated from strand 11 and then refolded in the absence of an added peptide, the chromophore absorption spectrum is quite different from that of native GFP, and the fluorescence quantum yield decreases by about a factor of three (58). Curiously, subsequent addition of a synthetic strand-11 peptide does not restore native absorption or fluorescence properties, indicating that order of operations is important. By chance, a sample containing this truncated protein with a synthetic strand-11 peptide

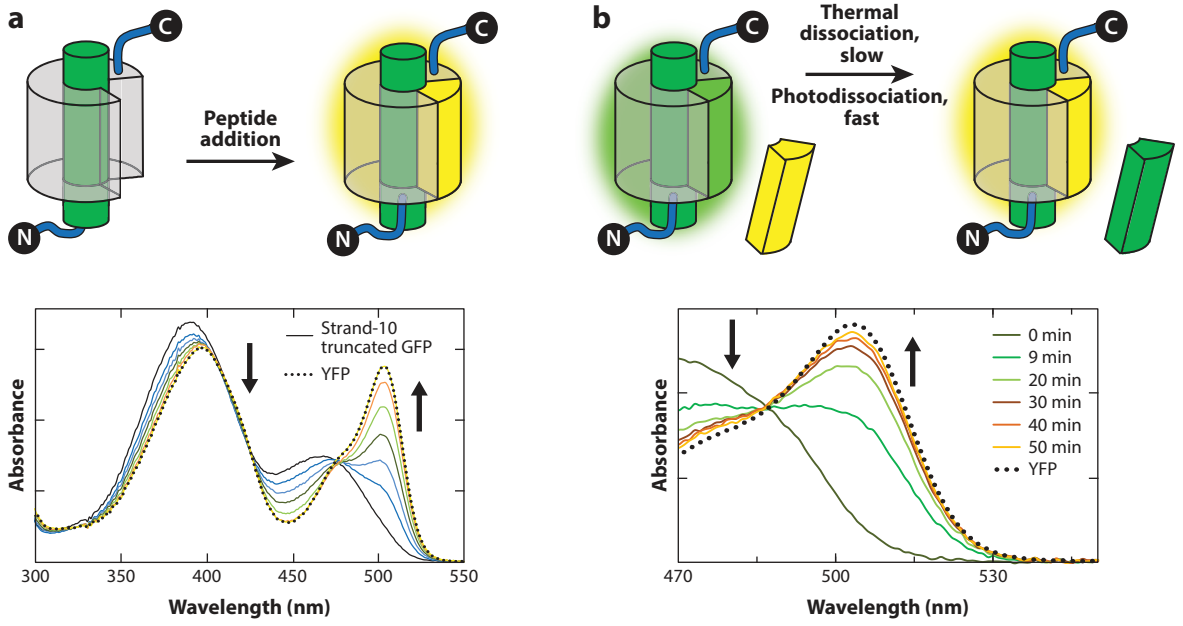

Figure 6

Strand binding and photodissociation of the strand-10 circularly permuted split green fluorescent protein (GFP). (*a*) When refolded in vitro, the truncated protein with strand 10 removed can bind synthetic peptides similar to strand 10. If the peptide contains the T203Y mutation responsible for the yellow color of yellow fluorescent protein (YFP), addition of aliquots of this peptide leads to a green-to-yellow color shift that signifies binding. Note that the structure of the truncated protein shown as a gray barrel is not currently known, although it does contain a mature chromophore. (*b*) In the presence of excess synthetic peptide containing the T203Y mutation, the proteolytically cleaved but still noncovalently attached native (T203) strand 10 does not dissociate spontaneously but does dissociate upon irradiation with blue light. The strand exchange is evident by a shift in the absorption spectrum similar to that observed by direct addition in panel *a*. Figure adapted with permission from Reference 26.

was exposed to light, and the native protein, indistinguishable from the original cut protein, was formed. Thus, it appeared that truncated GFP could be triggered by light to associate with peptides—an entirely unexpected result. The kinetics of this process were studied in detail.

Following up on the observations with strand-11 truncated GFP, we investigated a circularly permuted split GFP with the 10th β-strand at the N-terminus (26). The refolded strand-10 truncated protein (GFP11–9) had a different absorption spectrum and a very large (~30-fold) reduction in fluorescence quantum yield and, unlike the strand-11 truncated protein, was able to bind a synthetic strand-10 peptide without light irradiation. Synthetic peptides with mutations at the 203 position, such as T203Y responsible for the yellow color of the YFP family of GFPs, could also bind and tune the color of the chromophore (**Figure 6*a***). The color shift and large change in fluorescence quantum yield upon peptide binding were particularly convenient for following the kinetics and thermodynamics of the binding process, which were evaluated in depth. Surprisingly, in the presence of light and excess synthetic peptide, noncovalently bound strand 10 was replaced by the excess peptide, monitored by the green-to-yellow color change, implying that the native T203 peptide (green) photodissociated from the split protein and was replaced by the T203Y peptide (yellow) (**Figure 6*b***). The very large rate acceleration of strand exchange upon irradiation (at least 3,000-fold faster than in the dark) suggests that such split GFPs could be used as optogenetic tools, in addition to their traditional role for imaging. For example, light could

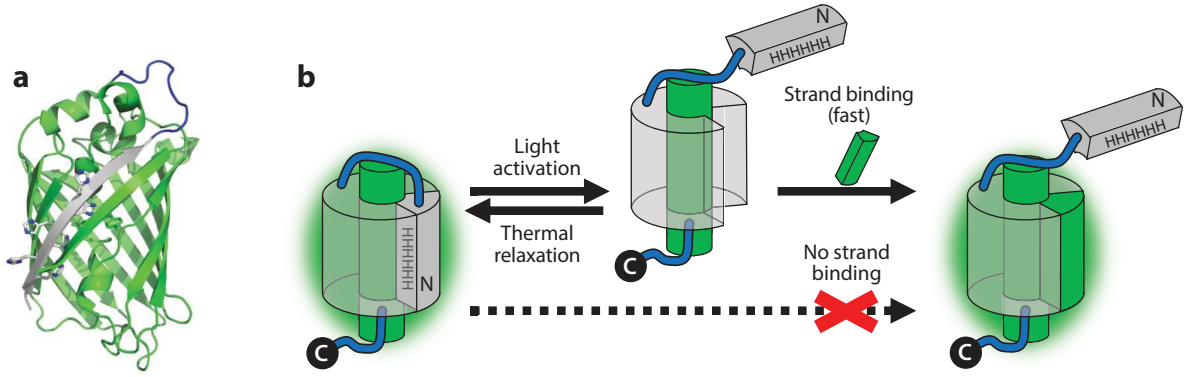

Figure 7

(*a*) Structure (PDB ID: 6B7R) (25) and (*b*) light activation of the strand-11 truncated protein. The N-terminal His tag (shown in *gray*) binds as a new β-strand to the vacant spot left by removal of the native 11th strand. Light irradiation displaces the bound His tag and allows for binding of added synthetic peptides (shown in *green*). Figure adapted with permission from Reference 25.

control reversible complementation, addressing a major limitation of BiFC discussed in detail in Section 3.3. Likewise, this potential optogenetic tool could act as a photocage by controlling either the release of an engineered, biologically relevant peptide or the activation of proteins such as enzymes and transcription factors in live cells with high spatial and temporal resolution. The primary limitation of this approach is the very low photodissociation quantum yield, as discussed in the next section.

The puzzling difference between the truncated split strand-10 and strand-11 proteins was resolved by obtaining the X-ray structure of the strand-11 truncated protein (**Figure 7*a***) (PDB ID: 6B7R) (25). This protein had an N-terminal His tag, commonly used as an affinity tag for protein purification, separated from the GFP barrel by a linker. Remarkably, the His tag and linker extend over the top of the protein barrel and slot precisely into the gap left by removing the C-terminal strand-11 peptide, creating a perfect β-strand with the six histidines alternating between inward- and outward-facing orientations in the immediate vicinity of the chromophore. The occlusion of the strand-11 binding site explains the phenomenological behavior discussed above: The His tag blocks binding of strand 11 to the truncated protein, and light irradiation displaces the bound His tag and allows for the binding of synthetic strand 11 [analogous to the strand exchange observed in the strand-10 circular permutant (**Figure 6*b***)] (**Figure 7*b***). As a result of the particular design of the strand-10 circular permutant, its His tag was removed along with strand 10, leaving open the peptide binding site in the truncated protein. By redesigning the circular permutant with strand 10 at the C-terminus and a His tag at the N-terminus, analogous to the strand-11 split protein variant, the His tag was shown by X-ray crystallography to bind in the empty slot left by removing strand 10 (PDB ID: 6B7T) (25); the resulting truncated protein bound the added synthetic strand-10 peptide at an accelerated rate upon light irradiation. Finally, Deng & Boxer (25) created "truly" truncated proteins that contained only the ten remaining β-strands and the internal α-helix by removing the His tag from both the strand-10 and strand-11 truncated proteins. Remarkably, these proteins were receptive to nonnative strands (e.g., the strand-11 truncated protein was shown to bind the strand-10 synthetic peptide), a promising result suggesting that this system can be engineered to reversibly bind biologically relevant peptides as both a sensor and an optogenetic tool.

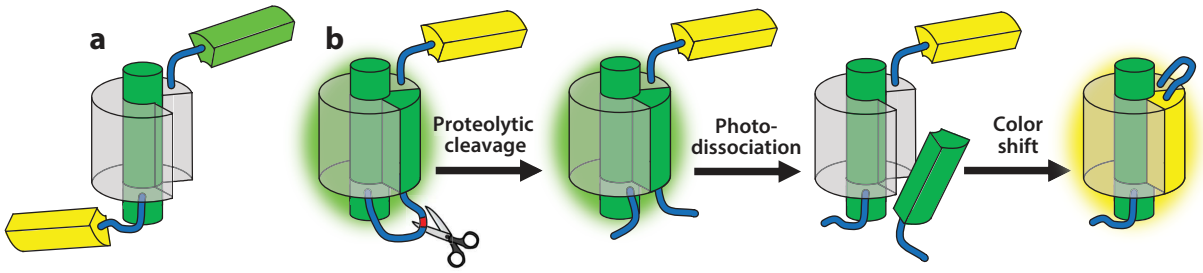

Figure 8

Two-tailed version of green fluorescent protein (GFP). (*a*) Cartoon illustrating the design of the two-tailed GFP. The rest of the barrel (strands 11 through 9) are flanked by two strand-10 peptides connected by linkers. A point mutation at position 203 on strand 10 leads to either a green (T203) or yellow (T203Y) fluorescent protein when bound. (*b*) Application of the two-tailed GFP engineered as a light-activated ratiometric protease sensor by combining light-driven photodissociation of the cut strand and strand replacement. Figure adapted with permission from Reference 27.

An interesting and related split GFP construct is the two-tailed version of GFP shown in **Figure 8*a*** (27). The strand-10 circularly permuted protein was modified with the native strand 10 as the N-terminus and an alternative version of strand 10 containing the T203Y mutation as the C-terminus. Depending on the linker length, either the green (native strand 10) or yellow (T203Y) strand completed the β-barrel upon protein expression and purification. Interesting variations in the green:yellow ratio were observed depending on whether the protein was isolated directly from *E. coli* or refolded from denaturing conditions in vitro. Taking advantage of the photodissociation of split GFP, a protease sensor was developed that could detect the presence of any specific protease by monitoring the change in color upon irradiation (**Figure 8*b***).

A number of other light-driven optogenetic tools based on fluorescent proteins that can report on important biological processes have been developed recently (163), along with related light-driven (but not GFP-derived) tools such as the light-oxygen-voltage sensing (LOV) domain (107), opsins (10), and several others reviewed elsewhere (18, 87, 136). A tool based on a split FP called photocleavable protein (PhoCl) was recently reported by Zhang et al. (162). Upon irradiation with violet light, green-to-red photoconversion of the chromophore occurs with concurrent irreversible peptide backbone cleavage. The noncovalently bound internal α-helix fragment then dissociates from the rest of the protein owing to an evolved low postcleavage peptide binding affinity. The PhoCl system was shown to allow spatiotemporal control of protein localization, enzyme activity, and gene expression with light.

4.4. Photochemistry of Split GFPs—Mechanism

Split GFP photodissociation has not yet been extensively exploited, largely owing to the low photodissociation quantum yield (<1% for photodissociation of strands 7, 10, or 11). To improve this quantum yield, rigorous mechanistic studies were performed. Initial results showed that the photodissociation rate rises linearly at low light intensity before plateauing, suggesting a two-step mechanism in which the first is light dependent and the second is a thermal process (26, 78). Further mechanistic insight came from studying both nonphotoswitchable and photoswitchable (E222Q mutant) circular permutants, which revealed that the light-dependent step is *cis-trans* isomerization of the chromophore followed by thermal strand dissociation (78). These findings link the properties of photodissociable split GFPs to reversibly photoswitchable GFPs that have been extensively engineered for super-resolution microscopy.

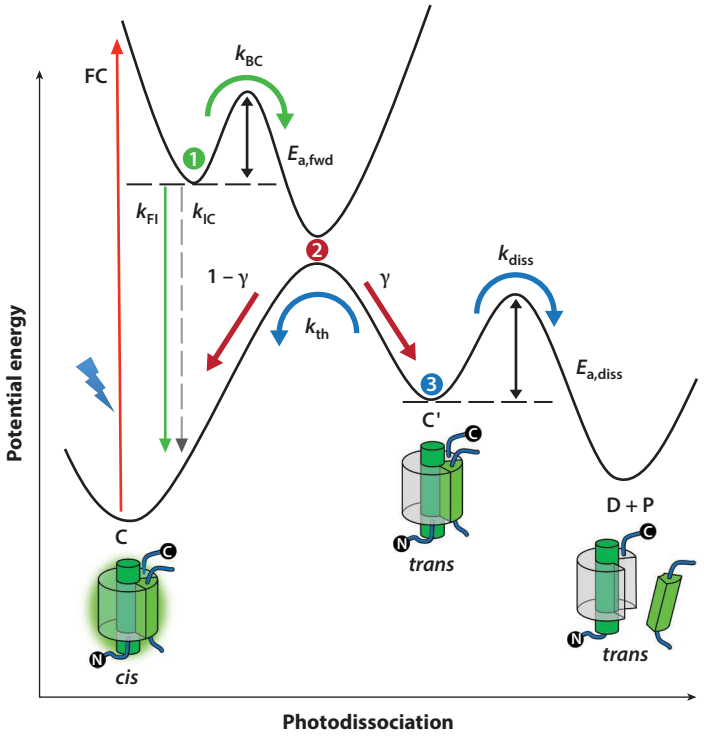

Figure 9

Potential energy curves for photodissociation, highlighting relevant parameters. Branching points are shown as circled numbers and are color coded to match their associated processes: ❶ represents the excited-state barrier partitioning fluorescence and isomerization; ❷ represents the photochemical funnel, which divides aborted from successful isomerization; and ❸ represents branching of strand dissociation and thermal relaxation. Abbreviations: C, noncovalently bound fluorescent protein complex with a *cis* chromophore in the ground electronic state; C', noncovalently bound fluorescent protein complex with a *trans* chromophore in the ground electronic state; D, truncated protein containing a *trans* chromophore in the ground electronic state with the dissociated strand removed; P, dissociated strand (peptide); γ, population branching ratio at the photochemical funnel; $E_{a,diss}$, energy barrier for thermal strand dissociation; $E_{a,fwd}$, energy barrier in the excited-state to reach photochemical funnel; FC, Franck-Condon excitation from the ground- to the excited-state; k_{BC}, rate constant for excited-state barrier crossing; k_{diss}, rate constant for strand dissociation; k_{FI}, rate constant for fluorescence; k_{IC}, rate constant for nonradiative internal conversion without passing through the photochemical funnel; k_{th}, rate constant for thermal relaxation from C' to C. Figure adapted with permission from Reference 78.

Further information on the energy landscape was obtained from the temperature dependence of photoactivation, strand dissociation, and fluorescence, with results summarized compactly in **Figure 9** (78). The first steps in this mechanism are similar to those found for other protein-based photoisomerizable systems such as rhodopsin and photoactive yellow protein. Following photoexcitation, there are several competing processes: fluorescence, nonradiative internal conversion, and a transition over an excited-state barrier (bottleneck 1) to a *cis-trans* isomerization step that occurs at a photochemical funnel (bottleneck 2). The (small) fraction of the population that makes it past the funnel with the chromophore in the *trans* state either decays back to *cis* over a ground-state barrier or leads to displacement of the cut strand (bottleneck 3). The strand displacement step was particularly informative, as it traps small populations that reach this point

through binding of excess synthetic peptide (not shown in **Figure 9**), a feature that is absent in related proteins. Each of the bottlenecks identified in this scheme provides a target for engineering the protein to enhance the partitioning toward strand photodissociation.

5. CONCLUSIONS AND OUTLOOK

Split FPs are versatile tools used to study numerous biophysical and biochemical processes. Additional properties such as light-activated fragment dissociation and binding-partner adaptability can address current limitations in the study of PPIs, such as irreversible complementation, as well as lay the foundation for exciting optogenetic applications. However, fundamental photophysical properties currently limit the potential of such applications. As with related issues of quantum yields and selectivity in other optogenetic systems, there does not yet exist a quantitative framework for predicting and achieving this engineering goal despite clear target bottlenecks for improvement. Directed evolution strategies using large randomized libraries or targeted rational design may be viable approaches for circumventing mechanistic bottlenecks; both approaches are currently underway. In combination with state-of-the-art simulations, it may be possible to elucidate the relationship between structure and energetics and begin formulating a unified design scheme for constructing a split FP–based optogenetic tool tailored to a specific application.

SUMMARY POINTS

1. Split proteins, both fluorescent and nonfluorescent, are extensively used to report on protein–protein interactions. Despite many drawbacks to the technique, proper and thorough controls can improve the confidence of data interpretation.
2. Beyond the study of protein–protein interactions, split fluorescent proteins are widely used for a myriad of other creative applications (e.g., a general interaction-based sensor, a sensor of various biological and biochemical processes, a molecular glue for controlled localization or materials design).
3. Synthetic control of split GFP allows for the study of basic photophysical properties of fluorescent proteins previously unobtainable by alternative methods.
4. Light sensitivity of split GFP transforms the system into a potential optogenetic tool, although current applications are limited owing to low quantum yields. Mechanistic insights will help guide future efforts to develop such tools.

DISCLOSURE STATEMENT

The authors are not aware of any affiliations, memberships, funding, or financial holdings that might be perceived as affecting the objectivity of this review.

ACKNOWLEDGMENTS

M.G.R. is supported by a Center for Molecular Analysis and Design fellowship. S.G.B.'s research program on GFP started with support from the Stanford Medical FEL Center, which was supported by the Office of Naval Research, where the original ultrafast measurements were made. Subsequently, this work has been generously supported by the NIH (NIGMS, currently R35

GM118044). We thank Jacob M. Kirsh, Chi-Yun Lin, and Samuel H. Schneider for insightful discussions and comments regarding this manuscript.

LITERATURE CITED

1. Acharya A, Bogdanov AM, Grigorenko BL, Bravaya KB, Nemukhin AV, et al. 2017. Photoinduced chemistry in fluorescent proteins: curse or blessing? *Chem. Rev.* 117:758–95
2. Avitabile E, Forghieri C, Campadelli-Fiume G. 2007. Complexes between herpes simplex virus glycoproteins gD, gB, and gH detected in cells by complementation of split enhanced green fluorescent protein. *J. Virol.* 81:11532–37
3. Bae C, Suchyna TM, Ziegler L, Sachs F, Gottlieb PA. 2016. Human PIEZO1 ion channel functions as a split protein. *PLOS ONE* 11:e0151289
4. Baird GS, Zacharias DA, Tsien RY. 1999. Circular permutation and receptor insertion within green fluorescent proteins. *PNAS* 96:11241–46
5. Baldwin RL. 2009. In memoriam: reflections on Fred Richards (1925–2009). *Protein Sci.* 18:682–85
6. Bale SS, Kwon SJ, Shah DA, Kane RS, Dordick JS. 2010. A GFP complementation system for monitoring and directing nanomaterial mediated protein delivery to human cellular organelles. *Biotechnol. Bioeng.* 107:1040–47
7. Barondeau DP, Putnam CD, Kassmann CJ, Tainer JA, Getzoff ED. 2003. Mechanism and energetics of green fluorescent protein chromophore synthesis revealed by trapped intermediate structures. *PNAS* 100:12111–16
8. Bertolaet BL, Knowles JR. 1995. Complementation of fragments of triosephosphate isomerase defined by exon boundaries. *Biochemistry* 34:5736–43
9. Blakeley BD, Chapman AM, McNaughton BR. 2012. Split-superpositive GFP reassembly is a fast, efficient, and robust method for detecting protein–protein interactions in vivo. *Mol. Biosyst.* 8:2036–40
10. Boyden ES, Zhang F, Bamberg E, Nagel G, Deisseroth K. 2005. Millisecond-timescale, genetically targeted optical control of neural activity. *Nat. Neurosci.* 8:1263–68
11. Cabantous S, Nguyen HB, Pédelacq JD, Koraichi F, Chaudhary A, et al. 2013. A new protein-protein interaction sensor based on tripartite split-GFP association. *Sci. Rep.* 3:2854
12. Cabantous S, Rogers Y, Terwilliger TC, Waldo GS. 2008. New molecular reporters for rapid protein folding assays. *PLOS ONE* 3:e2387
13. Cabantous S, Terwilliger TC, Waldo GS. 2005. Protein tagging and detection with engineered self-assembling fragments of green fluorescent protein. *Nat. Biotechnol.* 23:102–7
14. Cabantous S, Waldo GS. 2006. In vivo and in vitro protein solubility assays using split GFP. *Nat. Methods* 3:845–54
15. Callahan BP, Stanger MJ, Belfort M. 2010. Protease activation of split green fluorescent protein. *ChemBioChem* 11:2259–63
16. Chattoraj M, King BA, Bublitz GU, Boxer SG. 1996. Ultra-fast excited state dynamics in green fluorescent protein: multiple states and proton transfer. *PNAS* 93:8362–67
17. Chen M, Liu S, Li W, Zhang Z, Zhang X, et al. 2016. Three-fragment fluorescence complementation coupled with photoactivated localization microscopy for nanoscale imaging of ternary complexes. *ACS Nano* 10:8482–90
18. Christie JM, Gawthorne J, Young G, Fraser NJ, Roe AJ. 2012. LOV to BLUF: flavoprotein contributions to the optogenetic toolkit. *Mol. Plant* 5:533–44
19. Chu J, Zhang Z, Zheng Y, Yang J, Qin L, et al. 2009. A novel far-red bimolecular fluorescence complementation system that allows for efficient visualization of protein interactions under physiological conditions. *Biosens. Bioelectron.* 25:234–39
20. Chun W, Waldo GS, Johnson GV. 2007. Split GFP complementation assay: a novel approach to quantitatively measure aggregation of tau in situ: effects of GSK3β activation and caspase 3 cleavage. *J. Neurochem.* 103:2529–39
21. Cieri D, Vicario M, Giacomello M, Vallese F, Filadi R, et al. 2018. SPLICS: a split green fluorescent protein-based contact site sensor for narrow and wide heterotypic organelle juxtaposition. *Cell Death Differ.* 25:1131–45

22. Craggs TD. 2009. Green fluorescent protein: structure, folding and chromophore maturation. *Chem. Soc. Rev.* 38:2865–75
23. Cubitt AB, Woollenweber LA, Heim R. 1999. Understanding structure-function relationships in the *Aequorea victoria* green fluorescent protein. In *Methods in Cell Biology*, Vol. 58, ed. KF Sullivan, SA Kay, pp. 19–30. San Diego, CA: Academic
24. Demidov VV, Dokholyan NV, Witte-Hoffmann C, Chalasani P, Yiu H-W, et al. 2006. Fast complementation of split fluorescent protein triggered by DNA hybridization. *PNAS* 103:2052–56
25. Deng A, Boxer SG. 2018. Structural insight into the photochemistry of split green fluorescent proteins: a unique role for a His-tag. *J. Am. Chem. Soc.* 140:375–81
26. Do K, Boxer SG. 2011. Thermodynamics, kinetics, and photochemistry of β-strand association and dissociation in a split-GFP system. *J. Am. Chem. Soc.* 133:18078–81
27. Do K, Boxer SG. 2013. GFP variants with alternative β-strands and their application as light-driven protease sensors: a tale of two tails. *J. Am. Chem. Soc.* 135:10226–29
28. Enterina JR, Wu L, Campbell RE. 2015. Emerging fluorescent protein technologies. *Curr. Opin. Chem. Biol.* 27:10–17
29. Evdokimov AG, Pokross ME, Egorov NS, Zaraisky AG, Yampolsky IV, et al. 2006. Structural basis for the fast maturation of Arthropoda green fluorescent protein. *EMBO Rep.* 7:1006–12
30. Fan J-Y, Cui Z-Q, Wei H-P, Zhang Z-P, Zhou Y-F, et al. 2008. Split mCherry as a new red bimolecular fluorescence complementation system for visualizing protein–protein interactions in living cells. *Biochem. Biophys. Res. Commun.* 367:47–53
31. Fafarman AT, Boxer SG. 2010. Nitrile bonds as infrared probes of electrostatics in ribonuclease S. *J. Phys. Chem. B* 114:13536–44
32. Feinberg EH, Vanhoven MK, Bendesky A, Wang G, Fetter RD, et al. 2008. GFP reconstitution across synaptic partners (GRASP) defines cell contacts and synapses in living nervous systems. *Neuron* 57:353–63
33. Feng S, Sekine S, Pessino V, Li H, Leonetti MD, Huang B. 2017. Improved split fluorescent proteins for endogenous protein labeling. *Nat. Commun.* 8:370
34. Filonov GS, Verkhusha VV. 2013. A near-infrared BiFC reporter for in vivo imaging of protein-protein interactions. *Chem. Biol.* 20:1078–86
35. Fujii Y, Yoshimura A, Kodama Y. 2018. A novel orange-colored bimolecular fluorescence complementation (BiFC) assay using monomeric Kusabira-Orange protein. *BioTechniques* 64:153–61
36. Galarneau A, Primeau M, Trudeau L-E, Michnick SW. 2002. β-Lactamase protein fragment complementation assays as in vivo and in vitro sensors of protein–protein interactions. *Nat. Biotechnol.* 20:619–22
37. de Prat Gay G, Ruiz-Sanz J, Davis B, Fersht AR. 1994. The structure of the transition state for the association of two fragments of the barley chymotrypsin inhibitor 2 to generate native-like protein: implications for mechanisms of protein folding. *PNAS* 91:10943–46
38. Ghosh I, Hamilton AD, Regan L. 2000. Antiparallel leucine zipper-directed protein reassembly: application to the green fluorescent protein. *J. Am. Chem. Soc.* 122:5658–59
39. Han Y, Wang S, Zhang Z, Ma X, Li W, et al. 2014. In vivo imaging of protein–protein and RNA–protein interactions using novel far-red fluorescence complementation systems. *Nucleic Acids Res.* 42:e103
40. Heim R, Prasher DC, Tsien RY. 1994. Wavelength mutations and posttranslational autoxidation of green fluorescent protein. *PNAS* 91:12501–4
41. Hertel F, Mo GCH, Duwé S, Dedecker P, Zhang J. 2016. RefSOFI for mapping nanoscale organization of protein-protein interactions in living cells. *Cell Rep.* 14:390–400
42. Horstman A, Tonaco IA, Boutilier K, Immink RG. 2014. A cautionary note on the use of split-YFP/BiFC in plant protein-protein interaction studies. *Int. J. Mol. Sci.* 15:9628–43
43. Hu CD, Chinenov Y, Kerppola TK. 2002. Visualization of interactions among bZIP and Rel family proteins in living cells using bimolecular fluorescence complementation. *Mol. Cell* 9:789–98
44. Hu CD, Kerppola TK. 2003. Simultaneous visualization of multiple protein interactions in living cells using multicolor fluorescence complementation analysis. *Nat. Biotechnol.* 21:539–45

45. Huang Y-M, Banerjee S, Crone DE, Schenkelberg CD, Pitman DJ, et al. 2015. Toward computationally designed self-reporting biosensors using leave-one-out green fluorescent protein. *Biochemistry* 54:6263–73
46. Huang Y-M, Bystroff C. 2009. Complementation and reconstitution of fluorescence from circularly permuted and truncated green fluorescent protein. *Biochemistry* 48:929–40
47. Jach G, Pesch M, Richter K, Frings S, Uhrig JF. 2006. An improved mRFP1 adds red to bimolecular fluorescence complementation. *Nat. Methods* 3:597–600
48. Jackrel ME, Cortajarena AL, Liu TY, Regan L. 2010. Screening libraries to identify proteins with desired binding activities using a split-GFP reassembly assay. *ACS Chem. Biol.* 5:553–62
49. Jiang WX, Dong X, Jiang J, Yang YH, Yang J, et al. 2016. Specific cell surface labeling of GPCRs using split GFP. *Sci. Rep.* 6:20568
50. Johnsson N, Varshavsky A. 1994. Split ubiquitin as a sensor of protein interactions in vivo. *PNAS* 91:10340–44
51. Kaddoum L, Magdeleine E, Waldo GS, Joly E, Cabantous S. 2010. One-step split GFP staining for sensitive protein detection and localization in mammalian cells. *BioTechniques* 49:727–28
52. Kakimoto Y, Tashiro S, Kojima R, Morozumi Y, Endo T, Tamura Y. 2018. Visualizing multiple inter-organelle contact sites using the organelle-targeted split-GFP system. *Sci. Rep.* 8:6175
53. Kamiyama D, Sekine S, Barsi-Rhyne B, Hu J, Chen B, et al. 2016. Versatile protein tagging in cells with split fluorescent protein. *Nat. Commun.* 7:11046
54. Keem JO, Lee IH, Kim SY, Jung Y, Chung BH. 2011. Splitting and self-assembling of far-red fluorescent protein with an engineered beta strand peptide: application for alpha-synuclein imaging in mammalian cells. *Biomaterials* 32:9051–58
55. Kellermann SJ, Rath AK, Rentmeister A. 2013. Tetramolecular fluorescence complementation for detection of specific RNAs in vitro. *ChemBioChem* 14:200–4
56. Kellermann SJ, Rentmeister A. 2016. A genetically encodable system for sequence-specific detection of RNAs in two colors. *ChemBioChem* 17:895–99
57. Kellermann SJ, Rentmeister A. 2017. A FACS-based screening strategy to assess sequence-specific RNA-binding of Pumilio protein variants in *E. coli*. *Biol. Chem*. 398:69–75
58. Kent KP, Boxer SG. 2011. Light-activated reassembly of split green fluorescent protein. *J. Am. Chem. Soc.* 133:4046–52
59. Kent KP, Childs W, Boxer SG. 2008. Deconstructing green fluorescent protein. *J. Am. Chem. Soc.* 130:9664–65
60. Kent KP, Oltrogge LM, Boxer SG. 2009. Synthetic control of green fluorescent protein. *J. Am. Chem. Soc.* 131:15988–89
61. Kerppola TK. 2006. Design and implementation of bimolecular fluorescence complementation (BiFC) assays for the visualization of protein interactions in living cells. *Nat. Protoc.* 1:1278–86
62. Kerppola TK. 2006. Visualization of molecular interactions by fluorescence complementation. *Nat. Rev. Mol. Cell Biol.* 7:449–56
63. Kerppola TK. 2009. Visualization of molecular interactions using bimolecular fluorescence complementation analysis: characteristics of protein fragment complementation. *Chem. Soc. Rev.* 38:2876–86
64. Kikuchi N, Kolpashchikov DM. 2016. Split Spinach aptamer for highly selective recognition of DNA and RNA at ambient temperatures. *ChemBioChem* 17:1589–92
65. Kim YE, Kim Y-N, Kim JA, Kim HM, Jung Y. 2015. Green fluorescent protein nanopolygons as monodisperse supramolecular assemblies of functional proteins with defined valency. *Nat. Commun.* 6:7134
66. Knapp A, Ripphahn M, Volkenborn K, Skoczinski P, Jaeger KE. 2017. Activity-independent screening of secreted proteins using split GFP. *J. Biotechnol.* 258:110–16
67. Kodama Y, Hu CD. 2012. Bimolecular fluorescence complementation (BiFC): a 5-year update and future perspectives. *BioTechniques* 53:285–98
68. Kodama Y, Wada M. 2009. Simultaneous visualization of two protein complexes in a single plant cell using multicolor fluorescence complementation analysis. *Plant Mol. Biol.* 70:211–17

69. Kojima T, Karasawa S, Miyawaki A, Tsumuraya T, Fujii I. 2011. Novel screening system for protein–protein interactions by bimolecular fluorescence complementation in *Saccharomyces cerevisiae*. *J. Biosci. Bioeng*. 111:397–401
70. Köker T, Fernandez A, Pinaud F. 2018. Characterization of split fluorescent protein variants and quantitative analyses of their self-assembly process. *Sci. Rep.* 8:5344
71. Köker T, Tang N, Tian C, Zhang W, Wang X, et al. 2018. Cellular imaging by targeted assembly of hot-spot SERS and photoacoustic nanoprobes using split-fluorescent protein scaffolds. *Nat. Commun.* 9:607
72. Koraïchi F, Gence R, Bouchenot C, Grosjean S, Lajoie-Mazenc I, et al. 2018. High-content tripartite split-GFP cell-based assays to screen for modulators of small GTPase activation. *J. Cell Sci.* 131:jcs210419
73. Kost LA, Putintseva EV, Pereverzeva AR, Chudakov DM, Lukyanov KA, Bogdanov AM. 2017. Bimolecular fluorescence complementation based on the red fluorescent protein FusionRed. *Russ. J. Bioorg. Chem.* 42:619–23
74. Kudla J, Bock R. 2016. Lighting the way to protein-protein interactions: recommendations on best practices for bimolecular fluorescence complementation analyses. *Plant Cell* 28:1002–8
75. Lee YR, Park J-H, Hahm S-H, Kang L-W, Chung JH, et al. 2010. Development of bimolecular fluorescence complementation using Dronpa for visualization of protein–protein interactions in cells. *Mol. Imaging Biol.* 12:468–78
76. Leibly DJ, Arbing MA, Pashkov I, DeVore N, Waldo GS, et al. 2015. A suite of engineered GFP molecules for oligomeric scaffolding. *Structure* 23:1754–68
77. Leonetti MD, Sekine S, Kamiyama D, Weissman JS, Huang B. 2016. A scalable strategy for high-throughput GFP tagging of endogenous human proteins. *PNAS* 113:E3501–8
78. Lin CY, Both J, Do K, Boxer SG. 2017. Mechanism and bottlenecks in strand photodissociation of split green fluorescent proteins (GFPs). *PNAS* 114:E2146–55
79. Lindman S, Hernandez-Garcia A, Szczepankiewicz O, Frohm B, Linse S. 2010. In vivo protein stabilization based on fragment complementation and a split GFP system. *PNAS* 107:19826–31
80. Liu Z, Xing D, Su QP, Zhu Y, Zhang J, et al. 2014. Super-resolution imaging and tracking of protein–protein interactions in sub-diffraction cellular space. *Nat. Commun.* 5:4443
81. Luker KE, Smith MCP, Luker GD, Gammon ST, Piwnica-Worms H, Piwnica-Worms D. 2004. Kinetics of regulated protein-protein interactions revealed with firefly luciferase complementation imaging in cells and living animals. *PNAS* 101:12288–93
82. Magliery TJ, Wilson CGM, Pan W, Mishler D, Ghosh I, et al. 2005. Detecting protein–protein interactions with a green fluorescent protein fragment reassembly trap: scope and mechanism. *J. Am. Chem. Soc.* 127:146–57
83. Martell JD, Yamagata M, Deerinck TJ, Phan S, Kwa CG, et al. 2016. A split horseradish peroxidase for the detection of intercellular protein–protein interactions and sensitive visualization of synapses. *Nat. Biotechnol.* 34:774–80
84. Massoud TF, Paulmurugan R, Gambhir SS. 2010. A molecularly engineered split reporter for imaging protein-protein interactions with positron emission tomography. *Nat. Med.* 16:921–26
85. Michnick SW, Ear PH, Manderson EN, Remy I, Stefan E. 2007. Universal strategies in research and drug discovery based on protein-fragment complementation assays. *Nat. Rev. Drug Discov.* 6:569–82
86. Milech N, Longville BAC, Cunningham PT, Scobie MN, Bogdawa HM, et al. 2015. GFP-complementation assay to detect functional CPP and protein delivery into living cells. *Sci. Rep.* 5:18329
87. Möglich A, Moffat K. 2010. Engineered photoreceptors as novel optogenetic tools. *Photochem. Photobiol. Sci.* 9:1286–300
88. Morell M, Espargaró A, Avilés FX, Ventura S. 2007. Detection of transient protein–protein interactions by bimolecular fluorescence complementation: the Abl-SH3 case. *Proteomics* 7:1023–36
89. Morell M, Ventura S, Avilés FX. 2009. Protein complementation assays: approaches for the in vivo analysis of protein interactions. *FEBS Lett*. 583:1684–91
90. Müller J, Johnsson N. 2008. Split-ubiquitin and the split-protein sensors: chessman for the endgame. *ChemBioChem* 9:2029–38

91. Nguyen HB, Hung LW, Yeates TO, Terwilliger TC, Waldo GS. 2013. Split green fluorescent protein as a modular binding partner for protein crystallization. *Acta Crystallogr. Sect. D Biol. Crystallogr.* 69:2513–23
92. Nickerson A, Huang T, Lin L-J, Nan X. 2014. Photoactivated localization microscopy with bimolecular fluorescence complementation (BiFC-PALM) for nanoscale imaging of protein-protein interactions in cells. *PLOS ONE* 9:e100589
93. Nienhaus K, Nienhaus GU. 2016. Chromophore photophysics and dynamics in fluorescent proteins of the GFP family. *J. Phys. Condens. Matter* 28:443001
94. Ohashi K, Kiuchi T, Shoji K, Sampei K, Mizuno K. 2012. Visualization of cofilin-actin and Ras-Raf interactions by bimolecular fluorescence complementation assays using a new pair of split Venus fragments. *BioTechniques* 52:45–50
95. Oltrogge LM. 2015. *Using semi-synthetic fluorescent proteins to understand proton transfer*. PhD Thesis, Stanford Univ., Stanford, CA
96. Oltrogge LM, Wang Q, Boxer SG. 2014. Ground-state proton transfer kinetics in green fluorescent protein. *Biochemistry* 53:5947–57
97. Ottmann C, Weyand M, Wolf A, Kuhlmann J, Ottmann C. 2009. Applicability of superfolder YFP bimolecular fluorescence complementation in vitro. *Biol. Chem.* 390:81–90
98. Ozawa T, Natori Y, Sato M, Umezawa Y. 2007. Imaging dynamics of endogenous mitochondrial RNA in single living cells. *Nat. Methods* 4:413–19
99. Paige JS, Wu KY, Jaffrey SR. 2011. RNA mimics of green fluorescent protein. *Science* 333:642–46
100. Pakhomov AA, Martynov VI. 2008. GFP family: structural insights into spectral tuning. *Chem. Biol.* 15:755–64
101. Park E, Lee H-Y, Woo J, Choi D, Dinesh-Kumar SP. 2017. Spatiotemporal monitoring of *Pseudomonas syringae* effectors via type III secretion using split fluorescent protein fragments. *Plant Cell* 29:1571–84
102. Park K-H, Berrier C, Martinac B, Ghazi A. 2004. Purification and functional reconstitution of N- and C-halves of the MscL channel. *Biophys. J.* 86:2129–36
103. Pédelacq JD, Cabantous S, Tran T, Terwilliger TC, Waldo GS. 2006. Engineering and characterization of a superfolder green fluorescent protein. *Nat. Biotechnol.* 24:79–88
104. Pelletier JN, Campbell-Valois F-X, Michnick SW. 1998. Oligomerization domain-directed reassembly of active dihydrofolate reductase from rationally designed fragments. *PNAS* 95:12141–46
105. Pinaud F, Dahan M. 2011. Targeting and imaging single biomolecules in living cells by complementation-activated light microscopy with split-fluorescent proteins. *PNAS* 108:E201–10
106. Pu J, Zinkus-Boltz J, Dickinson BC. 2017. Evolution of a split RNA polymerase as a versatile biosensor platform. *Nat. Chem. Biol.* 13:432–38
107. Pudasaini A, El-Arab KK, Zoltowski BD. 2015. LOV-based optogenetic devices: light-driven modules to impart photoregulated control of cellular signaling. *Front. Mol. Biosci.* 2:18
108. Rackham O, Brown CM. 2004. Visualization of RNA–protein interactions in living cells: FMRP and IMP1 interact on mRNAs. *EMBO J.* 23:3346–55
109. Reid BG, Flynn GC. 1997. Chromophore formation in green fluorescent protein. *Biochemistry* 36:6786–91
110. Remington SJ. 2006. Fluorescent proteins: maturation, photochemistry and photophysics. *Curr. Opin. Struct. Biol.* 16:714–21
111. Remington SJ. 2011. Green fluorescent protein: a perspective. *Protein Sci.* 20:1509–19
112. Remy I, Michnick SW. 2004. A cDNA library functional screening strategy based on fluorescent protein complementation assays to identify novel components of signaling pathways. *Methods* 32:381–88
113. Richards FM. 1957. On the enzymatic activity of subtilisin-modified ribonuclease. *PNAS* 44:162–66
114. Robida AM, Kerppola TK. 2009. Bimolecular fluorescence complementation analysis of inducible protein interactions: effects of factors affecting protein folding on fluorescent protein fragment association. *J. Mol. Biol.* 394:391–409
115. Rodriguez EA, Campbell RE, Lin JY, Lin MZ, Miyawaki A, et al. 2017. The growing and glowing toolbox of fluorescent and photoactive proteins. *Trends Biochem. Sci.* 42:111–29
116. Rogers TA, Andrews GE, Jaeger L, Grabow WW. 2015. Fluorescent monitoring of RNA assembly and processing using the split-spinach aptamer. *ACS Synth. Biol.* 4:162–66

117. Rosenow MA, Huffman HA, Phail ME, Wachter RM. 2004. The crystal structure of the Y66L variant of green fluorescent protein supports a cyclization-oxidation-dehydration mechanism for chromophore maturation. *Biochemistry* 43:4464–72
118. Rossi F, Charlton CA, Blau HM. 1997. Monitoring protein–protein interactions in intact eukaryotic cells by β-galactosidase complementation. *PNAS* 94:8405–10
119. Sakamoto S, Terauchi M, Hugo A, Kim T, Araki Y, Wada T. 2013. Creation of a caspase-3 sensing system using a combination of split-GFP and split-intein. *Chem. Commun.* 49:10323–25
120. Saldaña C, Naranjo D, Coria R, Peña A, Vaca L. 2002. Splitting the two pore domains from TOK1 results in two cationic channels with novel functional properties. *J. Biol. Chem.* 277:4797–805
121. Santos-Aberturas J, Dörr M, Waldo GS, Bornscheuer UT. 2015. In-depth high-throughput screening of protein engineering libraries by split-GFP direct crude cell extract data normalization. *Chem. Biol.* 22:1406–14
122. Sarkar M, Magliery TJ. 2008. Re-engineering a split-GFP reassembly screen to examine RING-domain interactions between BARD1 and BRCA1 mutants observed in cancer patients. *Mol. Biosyst.* 4:599–605
123. Schmidt S, Adjobo-Hermans MJ, Wallbrecher R, Verdurmen WP, Bovée-Geurts PH, et al. 2015. Detecting cytosolic peptide delivery with the GFP complementation assay in the low micromolar range. *Angew. Chem. Int. Ed.* 54:15105–8
124. Shaner NC, Lambert GG, Chammas A, Ni Y, Cranfill PJ, et al. 2013. A bright monomeric green fluorescent protein derived from *Branchiostoma lanceolatum*. *Nat. Methods* 10:407–9
125. Shaner NC, Patterson GH, Davidson MW. 2007. Advances in fluorescent protein technology. *J. Cell Sci.* 120:4247–60
126. Shcherbakova DM, Baloban M, Emelyanov AV, Brenowitz M, Guo P, Verkhusha VV. 2016. Bright monomeric near-infrared fluorescent proteins as tags and biosensors for multiscale imaging. *Nat. Commun.* 7:12405
127. Shekhawat SS, Ghosh I. 2011. Split-protein systems: beyond binary protein–protein interactions. *Curr. Opin. Chem. Biol.* 15:789–97
128. Shen Y, Lai T, Campbell RE. 2015. Red fluorescent proteins (RFPs) and RFP-based biosensors for neuronal imaging applications. *Neurophotonics* 2:031203
129. Shiba K, Shimmel P. 1992. Functional assembly of a randomly cleaved protein. *PNAS* 89:1880–84
130. Shyu YJ, Hu CD. 2008. Fluorescence complementation: an emerging tool for biological research. *Trends Biotechnol.* 26:622–30
131. Shyu YJ, Liu H, Deng X, Hu CD. 2006. Identification of new fluorescent protein fragments for bimolecular fluorescence complementation analysis under physiological conditions. *BioTechniques* 40:61–66
132. Taniuchi H, Anfinsen CB, Sodja A. 1967. Nuclease-T: an active derivative of staphylococcal nuclease composed of two noncovalently bonded peptide fragments. *PNAS* 58:1235–42
133. Tchekanda E, Sivanesan D, Michnick SW. 2014. An infrared reporter to detect spatiotemporal dynamics of protein-protein interactions. *Nat. Methods* 11:641–44
134. Thomas EE, Pandey N, Knudsen S, Ball ZT, Silberg JJ. 2017. Programming post-translational control over the metabolic labeling of cellular proteins with a noncanonical amino acid. *ACS Synth. Biol.* 6:1572–83
135. Tilsner J, Linnik O, Christensen NM, Bell K, Roberts IM, et al. 2009. Live-cell imaging of viral RNA genomes using a Pumilio-based reporter. *Plant J.* 57:758–70
136. Tischer D, Weiner OD. 2014. Illuminating cell signalling with optogenetic tools. *Nat. Rev. Mol. Cell Biol.* 15:551–58
137. To TL, Schepis A, Ruiz-Gonzalez R, Zhang Q, Yu D, et al. 2016. Rational design of a GFP-based fluorogenic caspase reporter for imaging apoptosis in vivo. *Cell Chem. Biol.* 23:875–82
138. To TL, Zhang Q, Shu X. 2016. Structure-guided design of a reversible fluorogenic reporter of protein-protein interactions. *Protein Sci.* 25:748–53
139. Topell S, Hennecke J, Glockshuber R. 1999. Circularly permuted variants of the green fluorescent protein. *FEBS Lett.* 457:283–89
140. Tsien RY. 1998. The green fluorescent protein. *Annu. Rev. Biochem.* 67:509–44

141. Ueyama T, Kusakabe T, Karasawa S, Kawasaki T, Shimizu A, et al. 2008. Sequential binding of cytosolic phox complex to phagosomes through regulated adaptor proteins: evaluation using the novel monomeric Kusabira-Green system and live imaging of phagocytosis. *J. Immunol.* 181:629–40
142. Ullmann A, Jacob F, Monod J. 1967. Characterization by in vitro complementation of a peptide corresponding to an operator-proximal segment of the β-galactosidase structural gene of *Escherichia coli*. *J. Mol. Biol.* 24:339–43
143. Valencia-Burton M, McCullough RM, Cantor CR, Broude NE. 2007. RNA visualization in live bacterial cells using fluorescent protein complementation. *Nat. Methods* 4:421–27
144. Vidi P-A, Watts VJ. 2009. Fluorescent and bioluminescent protein-fragment complementation assays in the study of G protein-coupled receptor oligomerization and signaling. *Mol. Pharmacol.* 75:733–39
145. Waadt R, Schmidt LK, Lohse M, Hashimoto K, Bock R, Kudla J. 2008. Multicolor bimolecular fluorescence complementation reveals simultaneous formation of alternative CBL/CIPK complexes in planta. *Plant J.* 56:505–16
146. Walter M, Chaban C, Schütze K, Batistic O, Weckermann K, et al. 2004. Visualization of protein interactions in living plant cells using bimolecular fluorescence complementation. *Plant J.* 40:428–38
147. Wang L, Brock A, Herberich B, Schultz PG. 2001. Expanding the genetic code of *Escherichia coli*. *Science* 292:498–500
148. Wang S, Chen X, Chang L, Ding M, Xue R, et al. 2018. GMars-T enabling multimodal subdiffraction structural and functional fluorescence imaging in live cells. *Anal. Chem.* 90:6626–34
149. Wang S, Ding M, Chen X, Chang L, Sun Y. 2017. Development of bimolecular fluorescence complementation using rsEGFP2 for detection and super-resolution imaging of protein-protein interactions in live cells. *Biomed. Opt. Express* 8:3119–31
150. Wang S, Ding M, Xue B, Hou Y, Sun Y. 2018. Live cell visualization of multiple protein–protein interactions with BiFC rainbow. *ACS Chem. Biol.* 13:1180–88
151. Wang S, Ding M, Xue B, Hou Y, Sun Y. 2018. Spying on protein interactions in living cells with reconstituted scarlet light. *Analyst* 143:5161–69
152. Wehr MC, Laage R, Bolz U, Fischer TM, Grünewald S, et al. 2006. Monitoring regulated protein-protein interactions using split TEV. *Nat. Methods* 3:985–93
153. Wehr MC, Rossner MJ. 2016. Split protein biosensor assays in molecular pharmacological studies. *Drug Discov. Today* 21:415–29
154. Wiens MD, Campbell RE. 2018. Surveying the landscape of optogenetic methods for detection of protein–protein interactions. *Wiley Interdiscip. Rev. Syst. Biol. Med.* 10:e1415
155. Wu B, Chen J, Singer RH. 2014. Background free imaging of single mRNAs in live cells using split fluorescent proteins. *Sci. Rep.* 4:3615
156. Wyckoff HW, Hardman KD, Allewell NM, Inagami T, Johnson LN, Richards FM. 1967. The structure of ribonuclease-S at 3.5 Å resolution. *J. Biol. Chem.* 242:3984–88
157. Xia P, Liu X, Wu B, Zhang S, Song X, et al. 2014. Superresolution imaging reveals structural features of EB1 in microtubule plus-end tracking. *Mol. Biol. Cell* 25:4166–73
158. Yin C, Wang M, Lei C, Wang Z, Li P, et al. 2015. Phosphorylation-mediated assembly of a semisynthetic fluorescent protein for label-free detection of protein kinase activity. *Anal. Chem.* 87:6311–18
159. Yiu H-W, Demidov VV, Toran P, Cantor CR, Broude NE. 2011. RNA detection in live bacterial cells using fluorescent protein complementation triggered by interaction of two RNA aptamers with two RNA-binding peptides. *Pharmaceuticals* 4:494–508
160. Zetsche B, Volz SE, Zhang F. 2015. A split-Cas9 architecture for inducible genome editing and transcription modulation. *Nat. Biotechnol.* 33:139–42
161. Zhang J, Wang M, Tang R, Liu Y, Lei C, et al. 2018. Transpeptidation-mediated assembly of tripartite split green fluorescent protein for label-free assay of sortase activity. *Anal. Chem.* 90:3245–52
162. Zhang W, Lohman AW, Zhuravlova Y, Lu X, Wiens MD, et al. 2017. Optogenetic control with a photocleavable protein, PhoCl. *Nat. Methods* 14:391–94
163. Zhou XX, Chung HK, Lam AJ, Lin MZ. 2012. Optical control of protein activity by fluorescent protein domains. *Science* 338:810–14
164. Zimmer M. 2002. Green fluorescent protein (GFP): applications, structure, and related photophysical behavior. *Chem. Rev.* 102:759–81

Annual Review of Biophysics
Volume 48, 2019

Contents